JACS
JOURNAL OF THE AMERICAN CHEMICAL SOCIETY
Article
pubs.acs.org/JACS

Gold(I)-Catalyzed Allenyl Cope Rearrangement: Evolution from Asynchronicity to Trappable Intermediates Assisted by Stereoelectronic Switching

Dinesh V. Vidhani, Marie E. Krafft,[†] and Igor V. Alabugin*

Department of Chemistry & Biochemistry, Florida State University, Tallahassee, Florida 32306, United States

Supporting Information

ABSTRACT: Pericyclic reactions bypass high-energy reactive intermediates by synchronizing bond formation and bond cleavage. The present work offers two strategies for uncoupling these two processes and converting concerted processes into their "interrupted" versions by combining Au(I) catalysis with electronic and stereoelectronic factors. First, we show how the alignment of the C3−C4 bond with the adjacent π systems can control the reactivity and how the concerted scission of the central σ bond is prevented in the boat conformation. Second, the introduction of a fluorine atom at C3 also interrupts the sigmatropic shift and changes the rate-determining step of the interrupted cascade from the 6-endo-dig nucleophilic attack to the fragmentation of the central C3−C4 bond. Furthermore, this effect strongly depends on the relative orientation of the C−F bond toward the developing cationic center. The equatorial C−F bond has a much greater destabilizing effect on TS2 due to the more efficient through-bond interaction between the acceptor and the cationic π system. In contrast, the axial C−F bond is not aligned with the bridging C−C bonds and does not impose an equally strong deactivating stereoelectronic effect. These differences illustrate that the competition between concerted and interrupted pericyclic pathways can be finely tuned via a combination of structural and electronic effects modulated by conformational equilibria. The combination of Au(I) catalysis and C−F-mediated stereoelectronic gating delays the central bond scission, opening access to the interrupted Cope rearrangements and expanding the scope of this classic reaction to the design of new cascade transformations.

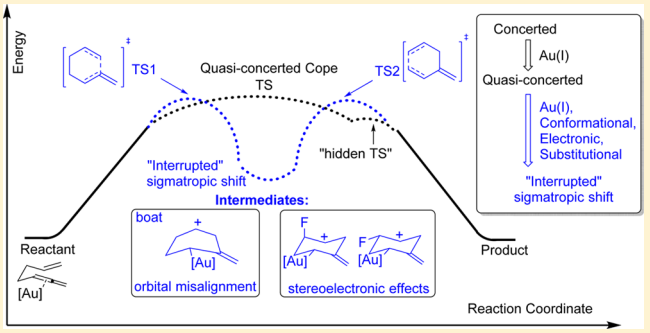

INTRODUCTION

Pericyclic reactions avoid the formation of high-energy reactive intermediates by synchronizing the bond-forming and bond-breaking steps. This feature accounts for many useful properties of these processes (stereospecificity, functional group compatibility, etc.) but also imposes limitations by closing the gates to numerous synthetic opportunities opened by interception of the putative intermediates. From this perspective, "interrupted", "aborted", and "hidden-TS" pericyclic reactions,[1] i.e., processes where the bond-forming and bond-breaking processes are fully or partially decoupled, have a special appeal.

In this context, the Cope rearrangement, a classic pericyclic process, offers a remarkably rich mechanistic playground. When the substrates contain radical stabilizing groups[2] or a strained subunit,[3] bond formation and bond cleavage are not perfectly synchronized. The potential energy surface (PES) of such sigmatropic rearrangements is characterized by the presence of a cyclic intermediate that is formed midway between the acyclic reactant and the product. A variety of electronic effects can transform the concerted process into a stepwise version, as illustrated in detail by Doering in his classic studies of "chameleonic" and "centauric" Cope transition states.[4−6] Subsequently, Schreiner pointed out the general trend that "*a nonconcerted [Cope rearrangement] reaction takes place when biradical intermediates are stabilized either by allyl or aromatic resonance*" (Figure 1) and expanded this concept to other interrupted processes "under the umbrella of a 'Cope' family".[7] Additionally, interactions with an external species can modify

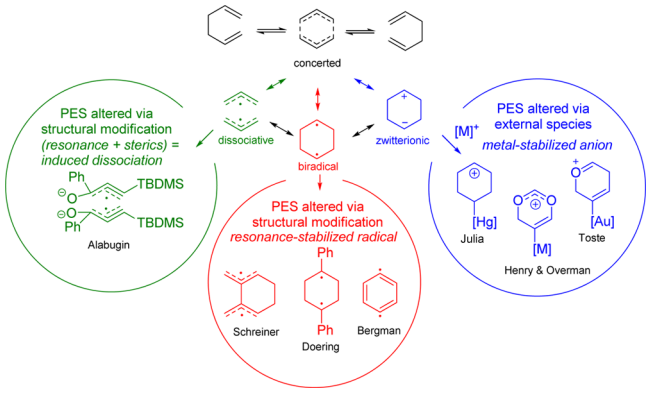

Figure 1. PES modification strategies in the Cope rearrangement.

Received: December 10, 2015
Published: February 5, 2016

DOI: 10.1021/jacs.5b12920
J. Am. Chem. Soc. 2016, 138, 2769−2779

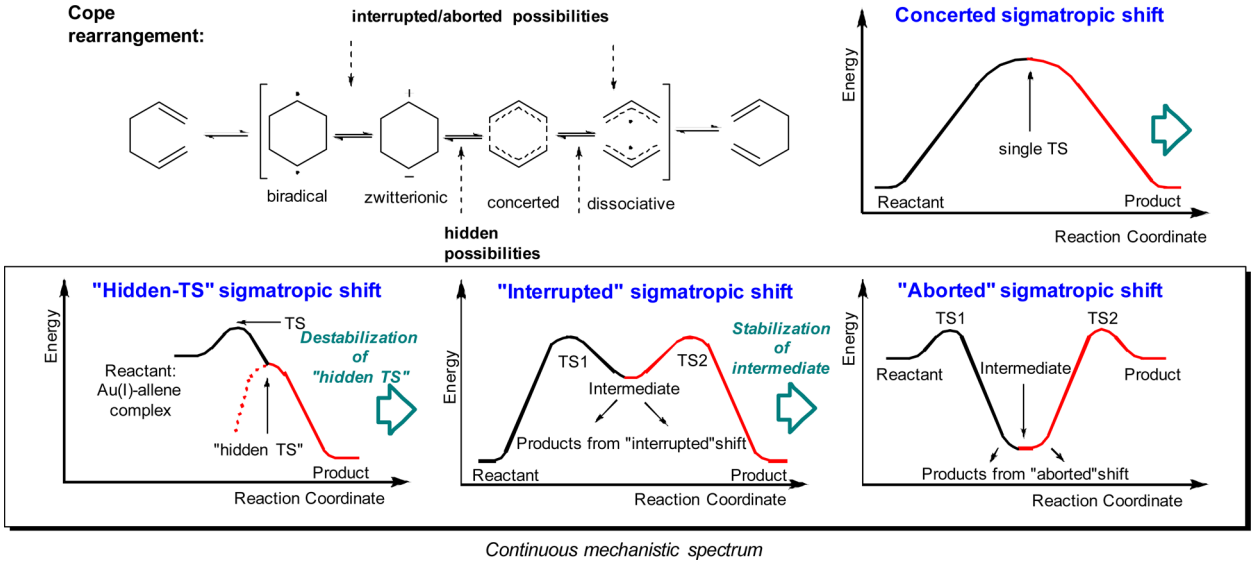

Figure 2. Evolution of the potential energy surface. Concerted, "hidden-TS", "interrupted", and "aborted" sigmatropic shifts are distinguished by the presence and stability of a second TS and intermediate cyclic species on the pericyclic TS.

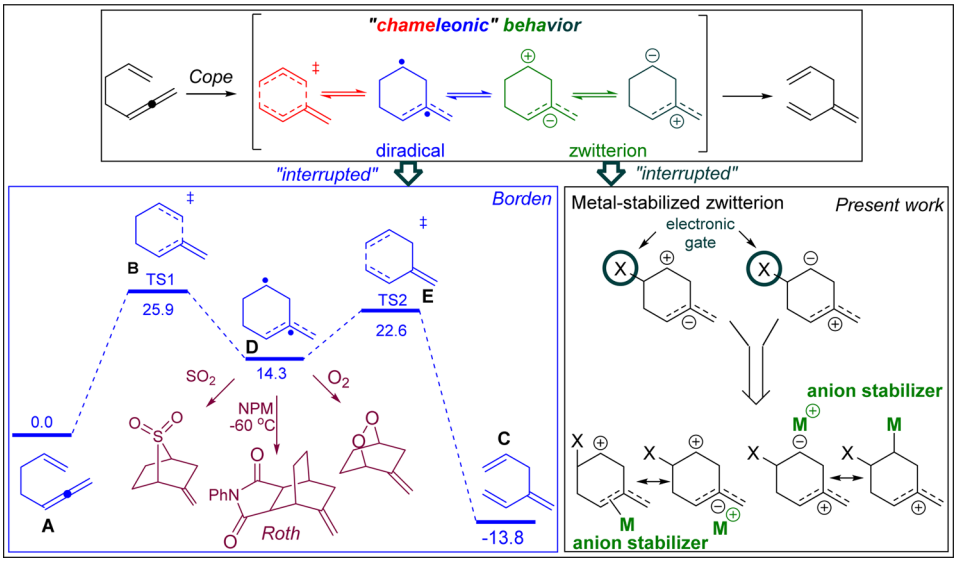

Figure 3. Exploration of the chameleonic transition state of the Cope rearrangement. (left) Reaction energy profile for the 1,2,6-heptatriene → 1,3,6-heptatriene Cope rearrangement. Intrinsic reaction coordinate calculations at the DFT level follow **A** → **B** → **C**, while the CASSCF method gives **A** → **B** → **D** → **E** → **C**. Structures in garnet color depict products emanating from trapping of intermediate **D**. (right) Possible effects of metal coordination on zwitterionic intermediates in the interrupted allenyl Cope rearrangement.

the potential energy surface to exhibit zwitterionic intermediates, as observed for metal-catalyzed propargyl Claisen rearrangement and propargyl ester rearrangement (vide infra).

Between the extremes of concerted and stepwise processes lies a scenario where an asynchronous process is on the verge of giving up its concertedness. Such a situation can lead to an inflection in the PES, which is often termed a "hidden transition state". Such a "hidden TS" can be located using energy gradients and aromaticity analysis.[8] Its presence suggests the potential for the transformation of a fully concerted reaction into an "interrupted" process involving discernible intermediates (Figure 2).[8] Depending on their stability, these diradical or zwitterionic intermediates either briefly "interrupt" or completely "abort" the sigmatropic process.[1,9] For an "interrupted" shift, the transient cyclic intermediates are higher in energy than the corresponding acyclic reactants/products. These cyclic intermediates can be trapped by another reaction without which the "interrupted" shift is invisible (i.e., the usual pericyclic products are formed). In the extreme case of the "aborted" shifts, the cyclic structures become the global minima on the sigmatropic shift PES and thus represent the final products of the rearrangement (Figure 2).[10]

The PES modification strategies have found important applications. For example, the transient generation of a metastable *p*-benzyne diradical intermediate in the Cope rearrangement of enediynes is the consequence of TS stabilization provided by π aromaticity (Figure 2). Because this species resides in a sufficiently deep potential energy well, it can be intercepted via radical[11] or ionic[12] processes of considerable value for synthesis, materials science, and the design of anticancer drugs (the Bergman cyclization).[13] The "aborted PES" is observed for [2,3] anionic shifts (the Wittig

DOI: 10.1021/jacs.5b12920
J. Am. Chem. Soc. 2016, 138, 2769–2779

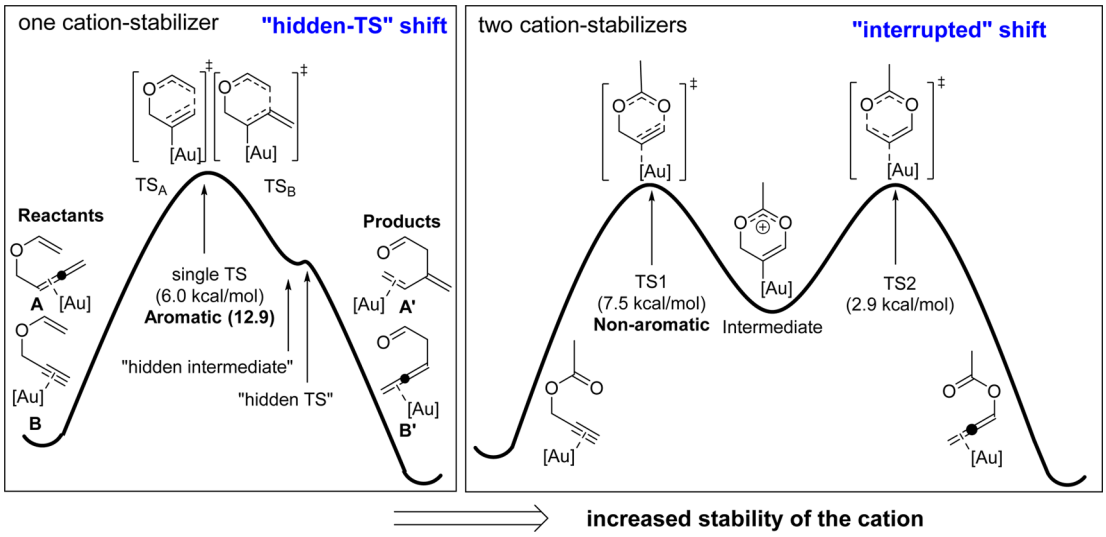

Figure 4. Schematic evolution of the potential energy surface as a function of cation stabilization. "Hidden-TS" and "interrupted" sigmatropic shifts are distinguished by the presence and stability of the second TS and the cyclic intermediate.

rearrangement), which can masquerade as anionic 5-endo cyclizations.[10,14]

Among the [3,3] sigmatropic rearrangements, the Cope rearrangement of the allenyl vinyl system has a special appeal because the flexibility of the transition state allows its "chameleonic" behavior to be harnessed, which presents an opportunity to study the unusual offshoots of the concerted process. In this context, the transition state of an uncatalyzed Cope rearrangement of acyclic 1,2,6-heptatriene already displays a "split personality" behavior, with signs of both diradical and concerted behavior. With the help of trapping agents such as oxygen and sulfur dioxide, Roth and co-workers[2a,6a,15] showed that the interrupted pathway involving a cyclic diradical intermediate competes with the concerted Cope rearrangement. Borden and co-workers illustrated the difficulty of computational analysis of such systems: a single transition state for the process **A** → **C** via **B** was found using density functional theory (DFT) calculations (Figure 3), but a diradical intermediate **E** was found to exist on the multiconfigurational complete active space self-consistent field (CASSCF) energy surface.[16] Borden further showed that the allylic resonance does not contribute to lowering the activation barrier. Instead, it is the formation of the stronger $C(sp^2)-C(sp^3)$ bond rather than the bridge $C(sp^3)-C(sp^3)$ bond that serves as the main source of this barrier lowering.

In our pursuit of a more general approach to "interrupted" and "aborted" variants of the Cope rearrangement and related sigmatropic shifts, we directed our attention to a strategy for the general modification of potential energy landscapes that involves complexation with *external* species, such as transition metal catalysts. We expected that such complexation can help in stabilizing the target zwitterionic intermediates (Figure 3). Indeed, metal coordination is well-suited for "interrupting" pericyclic reactions.[17] The available diversity of metals along with the additional fine-tuning by suitable ligands offers many opportunities for stabilizing unusual reactive intermediates, including unstable zwitterionic species. In this context, Au(I) species are electronically distinct because of their relative simplicity (the fully filled d subshell of Au^+) in comparison with other transition metals (Figure 4). This simplicity has earned Au(I) the reputation of a "well-dressed proton" that promotes electrophilic processes mostly by virtue of the creation of positive charge at the substrate. As with every analogy, this description is accurate only up to a point. Most importantly, interaction of the Au(I) catalyst with the substrate is significantly less exothermic and avoids the irreversible formation of vinyl cations in the early stages of the cascade. Furthermore, even despite this "simplicity", the Au(I) species can alter the potential energy landscape in a tunable fashion and give rise to "hidden TSs" and unstable intermediates. For instance, the Au(I)-catalyzed propargyl Claisen rearrangement and Au(I)-catalyzed allenyl vinyl ether rearrangement, which are topologically similar to the archetypical Cope rearrangement, proceed via highly asynchronous concerted paths that involve a "hidden TS".[8,18] Furthermore, the introduction of cation-stabilizing substituents converts a "hidden-TS" pathway into an "interrupted" shift. For instance, the alkenyl Cope rearrangement of substituted 1,5-dienes[19] and the 1,3 migration of the ester moiety in propargyl esters proceed via an "interrupted" path[20] that involves distinct six-membered intermediates (Figure 4).

In this work, we will focus on the metamorphosis of the PES caused by the presence of Au(I) and the combination of orbital alignment, orbital symmetry, and hyperconjugation in the Cope rearrangement of allenyl vinyl systems. A deeper understanding of the nature of the stereoelectronic factors that lead to the transformation of these processes would increase the future utility of Au(I) species, which are among the most powerful π-bond-activating catalysts.[21]

■ COMPUTATIONAL METHODS

The computational study for the present rearrangement was performed using the M06-2X/LANL2DZ method as implemented in Gaussian 03. Our previous study of the Rh(I)-catalyzed propargyl Claisen system showed that B3LYP, one of the most popular functionals used by organic chemists, gave poor correlation with the experimental results. In contrast, the M06-2X/LANL2DZ method gave excellent correlation with trends that were observed in the experimental data. Furthermore, the B3LYP functional is known to often underestimate activation energies[22] and provide unreliable thermochemical predictions in transition metal catalysis.[23] Between the 6-311++G(d,p) and LANL2DZ basis sets, the latter gave satisfactory results for the uncatalyzed rearrangement, as shown by

DOI: 10.1021/jacs.5b12920
J. Am. Chem. Soc. 2016, 138, 2769−2779

the comparison with the experimental results. Thus, all of the geometries were optimized using the M06-2X functional and the LANL2DZ basis set. To evaluate the effect of polarization, selected geometries were optimized using LANL2DZp, and the results were compared with the single-point energies calculated from the M06-2X/LANL2DZ geometries using a general basis set comprising 6-311++G(d,p) for nonmetals and Def2-TZVP for the Au(I) fragment.[24] Vibrational frequency calculations were performed to confirm that a given stationary point corresponded to a local minimum or a transition state on the potential energy surface. The transition states were located using the quadratic synchronous transit (QST3) method.[25] For structurally similar substrates, the QST-optimized geometries were modified and refined by restricted transition state searches using the Berny algorithm.

Delocalizing interactions were evaluated from M06-2X data using the NBO 3.0 software. Natural bond orbital (NBO) analysis[26] transforms the canonical delocalized molecular orbitals from DFT calculations into localized orbitals that are closely tied to chemical bonding concepts. Each of the localized NBO sets is complete and orthonormal. The filled NBOs describe the hypothetical, strictly localized Lewis structure. The interactions between filled and antibonding orbitals represent the deviation from the Lewis structure and can be used to measure delocalization.

RESULTS AND DISCUSSION

A. Uncatalyzed Cope Shift of 1,2,6-Heptatriene. Although the two transition state conformations, viz., chair and boat, significantly differ in structure and orbital alignment for the acyclic system, the restricted and unrestricted intrinsic reaction coordinate (IRC) calculations showed a concerted pathway containing a single TS for both TS conformations with both the M06-2X and B3LYP methods (see the Supporting Information for the IRC plots).[27] Additionally, the 6-311++G(d,p) bond parameters were found to be consistent with the LANL2DZ data while the LANL2DZ activation barrier was ~1 kcal/mol further away from the experimental value. The chair geometry provides the lowest-energy pathway (M06-2X/LANL2DZ: 30.9 kcal/mol). This value is closer to the experimental barrier (28.5 kcal/mol) than the previously reported B3LYP barrier (31.9 kcal/mol).[18,28] The barrier for the structurally deformed and considerably more dissociated boat conformation is much higher (43.9 kcal/mol (Figure 5).[29]

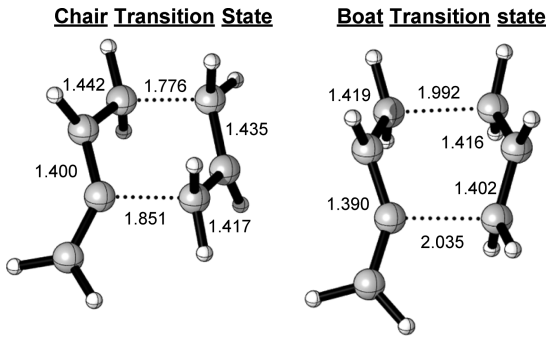

Figure 5. M06-2X/LANL2DZ-computed geometries of the chair and boat transition states for the uncatalyzed 1,2,6-heptatriene Cope rearrangement.

B. Au(I)-Catalyzed Rearrangement. The analysis of the uncatalyzed 1,2,6-heptatriene Cope rearrangement was particularly useful for benchmarking the previously reported experimental and theoretical data.[30] On the basis of the promising performance of the M06-2X functional for the uncatalyzed rearrangement and the recent reports of its success in describing several Au(I)-catalyzed rearrangements, we utilized this functional for all of the systems described in this work.[20] For the present system, we considered pathways emerging from (1) Au(I)−allene and (2) Au(I)−alkene complexes. At the M06-2X/LANL2DZ level of theory, the $AuPMe_3$ cation forms a 2.0 kcal/mol more stable complex with the alkene than with the allene.[31] However, even though Au(I)−allene coordination produces a higher-energy complex, the greater nucleophilicity of the alkenic π bond may decrease the cyclization barrier and compensate for such reactant destabilization.

1. Au(I)−Allene Pathway. Boat versus Chair: Conformational Interruption of a Pericyclic Process. Analogously to the uncatalyzed rearrangement, the transition state can adopt a chair or boat conformation. Although Au coordination decreased the barrier by ~20 kcal/mol in comparison with that for the noncatalyzed rearrangement for both pathways, the chair TS is still significantly lower in energy than the boat TS (10.6 vs 17.0 kcal/mol). However, if the chair path were prohibited by a structural constraint, the boat TS would certainly present a viable alternative rearrangement path.

The key process that controls multiple pathways is the C3−C4 bond scission. In a concerted process, this step is synchronized with the other bond-forming and bond-cleaving processes. In an "interrupted" shift, it is delayed and occurs in the last step, after the cyclic intermediate is formed. In contrast to the noncatalyzed version, the C3−C4 bond cleavage is not synchronized with other bond-forming and bond-scission processes. As a result, both TS conformations largely retain the integrity of the C3−C4 bond (Figure 6).[32] The chair TS is

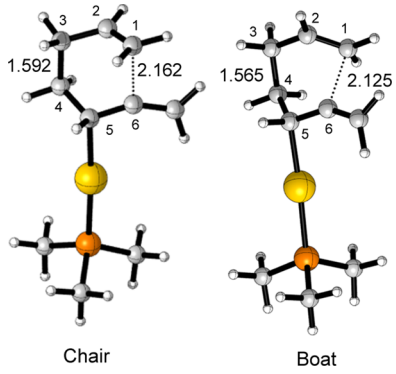

Figure 6. M06-2X/LANL2DZ-computed geometries of the chair and boat transition state conformations originating from $Me_3PAu(I)$−allene coordination. Bond distances for the σ(C3−C4) bond scission and the σ(C1−C6) bond formation are shown in Å.

less distorted (H−C3−C4−H dihedral angle = 170° vs 162° for the boat). Furthermore, the calculated geometries reflect a slightly greater elongation of the C3−C4 bond for the chair than for the boat (1.592 vs 1.565 Å). In parallel, the C2−C3 bond shows greater double-bond character in the chair conformation (1.484 Å vs 1.495 Å for the boat). The relatively short C3−C4 bond distances indicate that the TS geometries structurally correspond to the first step of the "interrupted" shift, the 6-endo nucleophilic attack of the alkene moiety.

The chair TS leads to a classical carbocation at the terminal point of the 6-endo trajectory. This species, however, is not an energy minimum: it undergoes nearly spontaneous collapse to the final Cope product with an extremely low lying TS2 (barrier = 0.1 kcal/mol) corresponding to the σ(C3−C4)

DOI: 10.1021/jacs.5b12920
J. Am. Chem. Soc. 2016, 138, 2769−2779

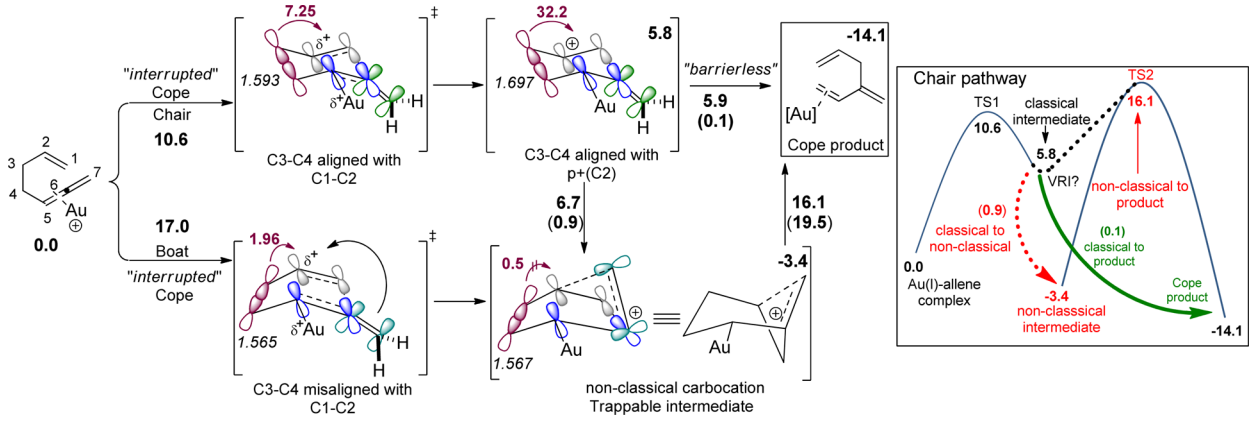

Figure 7. Reactions of the boat and chair conformers of the $Me_3PAu(I)$−allene complex. Values above the arrows correspond to activation energies calculated at the M06-2X/LANL2DZ level relative to the $Me_3PAu(I)$−allene complex. Values in parentheses correspond to the activation barriers calculated relative to the preceding structures. Values within the boxes correspond to the equilibrium values calculated relative to the $Me_3PAu(I)$−allene complex. Values in maroon indicate NBO interaction energies in kcal/mol, and values in italics indicate bond distances in Å.

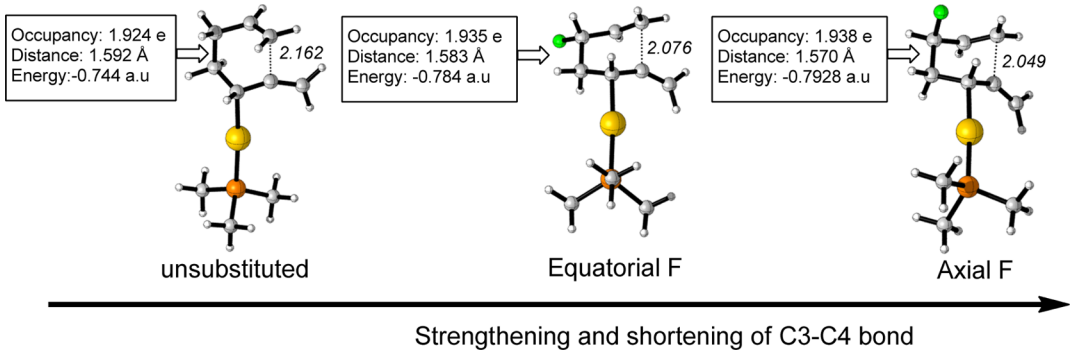

Figure 8. M06-2X/LANL2DZ-computed TS geometries of unsubstituted, equatorial-F-substituted, and axial-F-substituted substrates. The values in the boxes correspond to σ(C3−C4) bond occupancies, distances, and energies.

fragmentation. The nearly spontaneous breach of the σ(C3−C4) bond stems from the chair geometry (C1−C2−C3−C4 dihedral angle = 82°), which perfectly aligns the breaking σ(C3−C4) bond with the empty π^*(C1−C2) orbital [σ(C3−C4) → π^*(C1−C2) NBO interaction energy = 7.3 kcal/mol]. Furthermore, we found another low-energy path (0.9 kcal/mol) connecting the classical and nonclassical carbocations (Figure 7).

The scenarios of common intermediates connecting two different products have been extensively discussed in the literature.[33] In the present case, the classical cation represents the PES bifurcation point that gives a Cope product on one side and a bicyclic carbocation on the other side. Because this bicyclic carbocation is more stable than the reactant, its formation could be considered an aborted sigmatropic shift. However, this product can rearrange further to the even more stable normal Cope product, albeit via a path with a relatively high barrier (19.5 kcal/mol) that requires scission of the σ(C3−C4) bond.

In summary, the impact of Au(I) depends on the orientation of the orbitals (Figures 6 and 7). Even though the increased electrophilicity of the π^*(C5−C6) orbital in the complex with the cationic Au species uniformly accelerates all of the Au-mediated transformations of the substrate, the boat conformation misaligns the σ(C3−C4) and π(C1−C2) orbitals and prevents the scission of the σ(C3−C4) bond. As a result, the subsequent step leading to the normal Cope product is a high-energy pathway (16.1 kcal/mol from the reactant and 19.5 from the nonclassical intermediate). On the basis of these results, one can envision synthetic routes to a variety of bicyclic compounds originating from trapping of this intermediate via sufficiently fast processes.

Furthermore, in the following section, we will describe additional factors that can be used synergistically with the above conformational effects to interrupt a Au-catalyzed Cope rearrangement. They originate from the increased polarization of the organic substrate that distinguishes the Au-catalyzed Cope reaction from its classic thermal counterpart and leads to significant charge separation and accumulation in ionic intermediates and transition states. In particular, the appearance of an inflection along the PES corresponding to the fragmentation of the σ(C3−C4) bond presents an opportunity to disrupt the concerted reaction if one can use appropriately positioned polar substituents as stereoelectronic control elements. The following section will illustrate the potential of this approach.

Fluorine Substitution as an Additional Control Element in the Design of Interrupted/Aborted Cope Reactions. The unique stereoelectronic features of organofluorine compounds[34] have been used in areas ranging from organic reaction design,[35] biotechnology,[36] and catalysis[37] to materials and polymer sciences.[38] We have investigated whether the lability of the σ(C3−C4) bond in the chair TS of the 1,2,6-heptatriene Cope rearrangement can be controlled by fluorine substitution. Indeed, installing fluorine at C3 significantly modifies the PES by strengthening the σ(C3−C4) bond. In

DOI: 10.1021/jacs.5b12920
J. Am. Chem. Soc. 2016, 138, 2769−2779

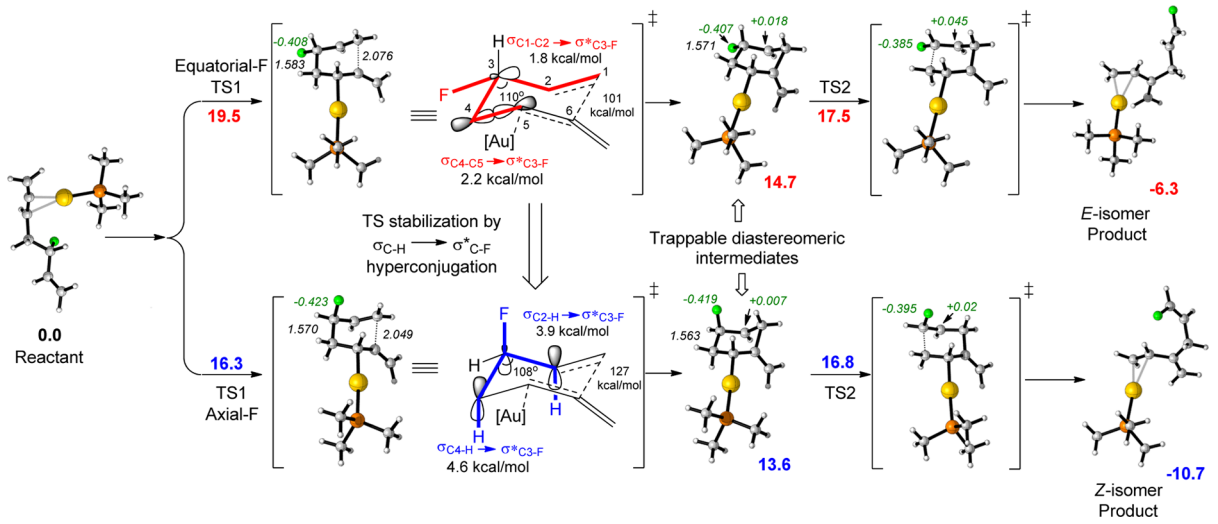

Figure 9. Comparison of the axial-F and equatorial-F pathways for the $Me_3PAu(I)$−allene complex. Geometries were optimized at the M06-2X/LANL2DZ level. Values near the arrows correspond to the activation barriers calculated relative to the $Me_3PAu(I)$−allene reactant. Values beside the structures correspond to their energies in kcal/mol relative to the $Me_3PAu(I)$−allene reactant. Values in green and black italics correspond to NBO charges in *e* and distances in Å, respectively. Values in black correspond to hyperconjugation interactions.

particular, the fluorinated substrates show higher σ(C3−C4) populations, shorter σ(C3−C4) bond distances, and lower energy of the σ(C3−C4) NBO (Figure 8) in comparison with the unsubstituted substrate. Furthermore, the effect of fluorine is stereoelectronic, and the properties of the two diastereomeric cyclic intermediates, differentiated by the axial/equatorial orientation of the fluorine atom, are remarkably different.

Among the two orientations, the axial isomer shows hyperconjugation in which the the axial σ^*(C3−F) orbital is aligned with the two better donors, the σ(C4−H) and σ(C2−H) bonds [NBO interaction energies: σ(C4−H) → σ^*(C3−F), 4.6 kcal/mol, σ(C2−H) → σ^*(C3−F), 3.9 kcal/mol]. On the other hand, the equatorial σ^*(C3−F) C−F isomer is aligned with the poor donors, the σ(C1−C2) and σ(C4−C5) bonds, which are depleted by their proximity to the cationic center [σ(C1−C2) → σ^*(C3−F), 1.8 kcal/mol; σ(C4−C5) → σ^*(C3−F), 2.2 kcal/mol]. This stereoelectronic effect can be considered as an extended version of the gauche effect that is comparable in magnitude to the destabilization imposed by an equatorial C−F bond via double hyperconjugation of the equatorial "hyperconjomer" of δ-cyclohexyl cation.[39]

As a result, the axial-F conformer shows a shorter (1.570 Å) and stronger σ(C3−C4) bond than the equatorial conformer (Figure 9). Furthermore, the lowest-energy axial-F pathway has a different rate-limiting step: the TS for the σ(C3−C4) bond scission has a slightly higher absolute energy than the cyclization TS (16.8 vs 16.3 kcal/mol). In contrast, the rearrangement of the equatorial conformer proceeds via a rate-limiting cyclization step. The corresponding 6-endo TS is ∼2 kcal/mol higher in energy than the fragmentation TS. Of the two orientations, the axial conformer gives the thermodynamically more stable *Z* isomer of the product (−10.7 kcal/mol).

In comparison with the unsubstituted substrate, the installation of fluorine at C3 raises the barrier for the C3−C4 bond scission in the cyclic intermediate from 0.1 to ∼3 kcal/mol. This increase makes the interruption of the concerted [3,3] shift more likely even for the chair geometries. Cooperative effects of several optimally positioned substituents may provide even stronger perturbations. Such stereoelectronic tuning of the Au(I)-catalyzed Cope shift is expected to open new avenues for intercepting cyclic intermediates.

2. Au(I)−Alkene Pathway. The nature of this rearrangement is significantly different from the previously discussed pathways. On one hand, the allenic π bond (NBO energy = −0.418 au) is less nucleophilic than the alkene. On the other hand, its reaction with the electrophilic Au(I)−alkene complex results in an allyl carbocation.[40] This scenario is similar to the thermal Cope rearrangement of 1,2,6-heptatriene proceeding via a diradical intermediate consisting of a secondary radical and an allyl radical.[2,18] The TSs of such allyl radicals do not benefit from resonance because the adjacent π bond is orthogonal to the singly occupied p orbital (Figure 10). Thus, one can expect that the TS leading to the allyl cation part of the Au(I)-stabilized zwitterion can benefit from resonance only if the terminal allenic π bond is distorted in such a way that it takes part in the stabilization process.

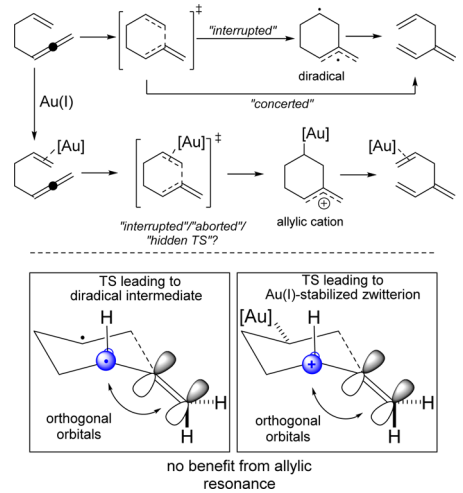

Figure 10. Possibility of interruption in the uncatalyzed and $Me_3PAu(I)$-catalyzed rearrangements of 1,2,6-heptatriene with $Me_3PAu(I)$ coordinating to the alkene.

DOI: 10.1021/jacs.5b12920
J. Am. Chem. Soc. 2016, 138, 2769−2779

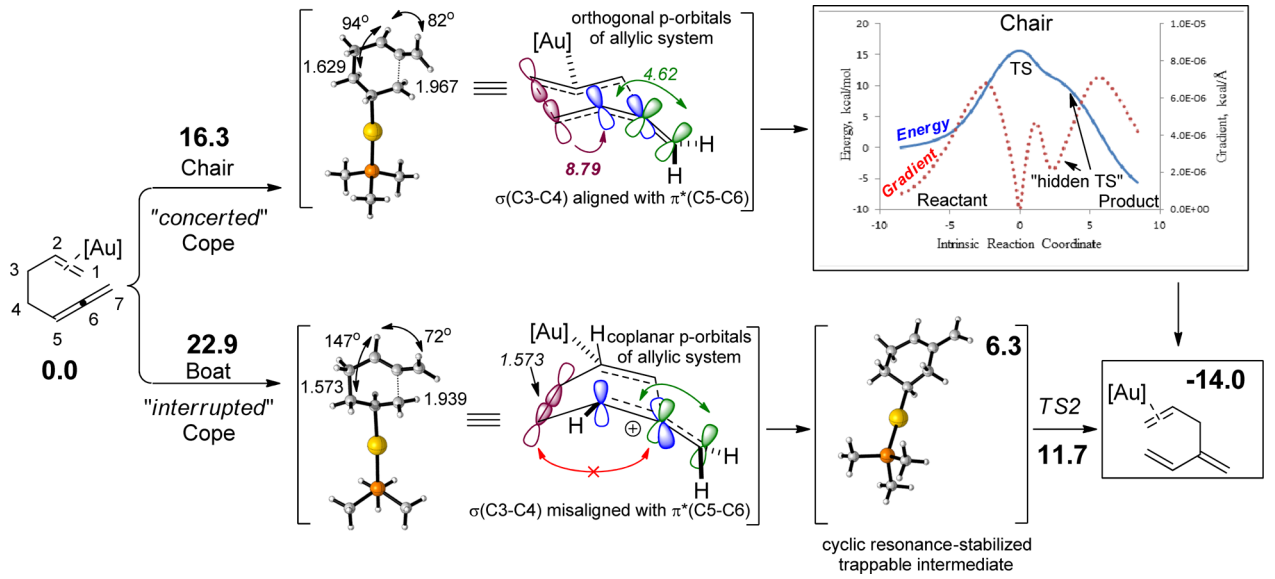

Figure 11. Scheme showing the chair and boat conformations emanating from the $Me_3PAu(I)$–alkene pathway. The geometries were optimized at the M06-2X/LANL2DZ level. The values over the arrows correspond to the respective barriers, whereas values near the structures correspond to reaction energies. The inset at the top right corresponds to the IRC calculation, showing the energy and gradient curves for the chair conformation.

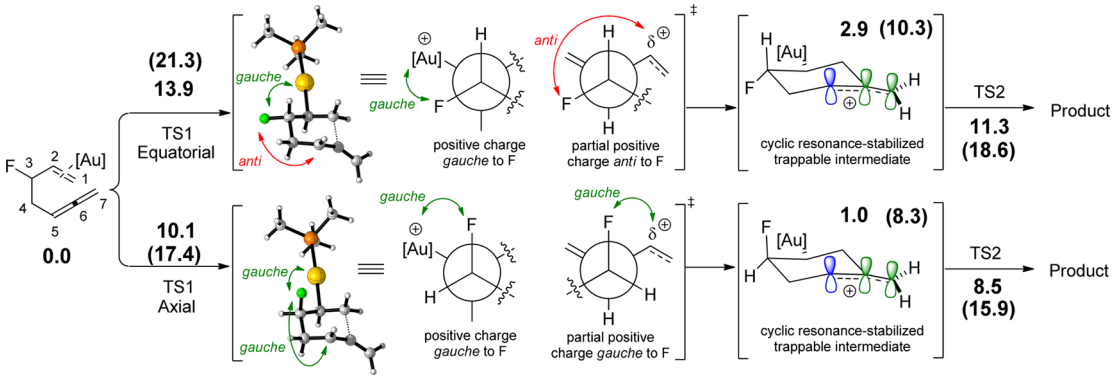

Figure 12. Scheme depicting axial-F and equatorial-F chair Cope pathways for the $Me_3PAu(I)$–alkene complex. The geometries were optimized at the M06-2X/LANL2DZ level. Values over the arrows correspond to activation barriers, whereas those beside the structures correspond to the equilibrium energies. Values in parentheses correspond to energies calculated from the most stable $Me_3PAu(I)$–allene complex.

In analogy with the diradical case, the Au(I)-bound zwitterionic chair TS mostly retains the orthogonality of the π(C5–C6) and π(C6–C7) orbitals (H–C5–C7–H dihedral angle = 82°) that inhibits the development of the allylic resonance [π(C6–C7) → π(C5–C6) = 4.6 kcal/mol] (Figure 11, top). However, this geometry (C3–C4–C5–H dihedral angle = 94°) also allows relatively efficient σ(C3–C4) → π(C5–C6) delocalization (8.5 kcal/mol), which weakens the σ(C3–C4) bond (1.629 Å). This orbital communication keeps the process on a nearly concerted path: only a gradient analysis (red dotted curve in the Figure 11 inset) could find the "hidden TS" as an inflection with the geometric parameters indicative of the σ(C3–C4) bond scission.

In contrast, the warped-boat geometry removes the orthogonality of the π(C5–C6) and π(C6–C7) orbitals, permitting the allylic resonance (Figure 11, bottom). Furthermore, the distortion misaligns the σ(C2–C3) and π(C5–C6) orbitals and also inhibits σ(C3–C4) → π(C5–C6) delocalization (1.2 kcal/mol only). The first effect stabilizes the cyclic intermediate, whereas the second effect destabilizes the TS for conversion of this intermediate to the final product. Both effects favor interruption of the pericyclic path. Indeed, the scission of the σ(C2–C3) bond (1.573 Å) is averted, leading to an "interrupted" shift with a fully developed allylically stabilized cyclic carbocation.

In analogy with the uncatalyzed rearrangement of 1,2,6-heptatriene, the lowest-energy chair TS for the Cope rearrangement of the Au(I)–alkene complex also exhibits negligible allylic delocalization. The boat TS remains higher in energy (22.9 kcal/mol) than the chair TS (16.3 kcal/mol) even despite the early development of allylic resonance stabilization in the cationic transition state connecting 1,2,6-heptatriene with the incipient cyclic intermediate. However, the difference in the energies of the chair and boat conformations is dramatically decreased in comparison with the thermal rearrangement ($\Delta\Delta E^{\ddagger}$ = 6.6 vs 13.0 kcal/mol). This change reiterates that significant modification of the electronic nature of the Cope TS is possible in its Au-catalyzed versions.

Fluorine Gate in the Au(I)–Alkene Pathway: Gauche Effect. The "gauche effect" is the conformational preference for the gauche orientation of vicinal polar bonds.[35] It becomes prominent in organofluorine compounds, where the gauche conformation is stabilized by hyperconjugative σ(C–H) → σ^*(C–F) interactions and electrostatic effects.[41,42] Practically,

DOI: 10.1021/jacs.5b12920
J. Am. Chem. Soc. 2016, 138, 2769–2779

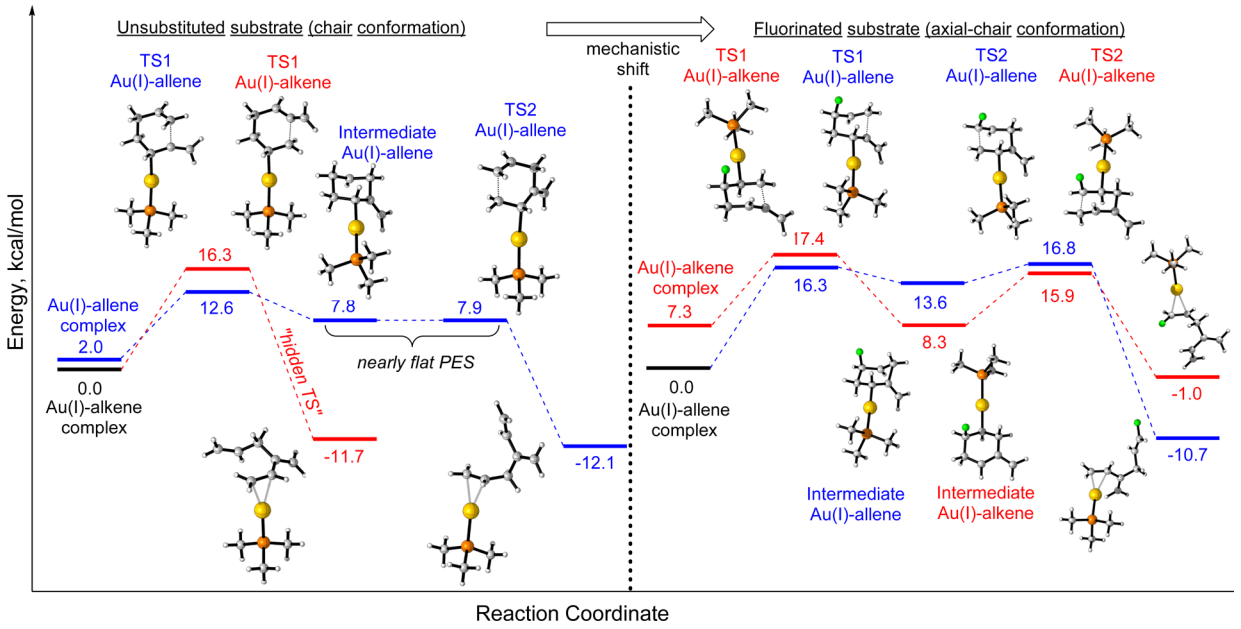

Figure 13. Curtin–Hammett analysis of unsubstituted and fluorinated substrates. The lowest-energy pathways are shown in blue. Geometries were optimized at the M06-2X/LANL2DZ level.

the gauche effect can facilitate access to conformations that are challenging to obtain by traditional steric locking strategies.[35−39,43]

In the present scenario, Au(I)−alkene coordination puts fluorine in the immediate vicinity of a positively charged Au(I) species and a developing positive charge on C5 (Figure 12). Under these circumstances, the 6-endo-trig nucleophilic attack by the allenic π system generates two diastereomeric intermediates. The chair transition state TS1 leading to the equatorial diastereomer contains a fluorine atom that is anti to the developing empty orbital on C5. The resulting destabilization of the developing positive charge raises the barrier (13.9 kcal/mol). Furthermore, the equatorial orientation of fluorine destabilizes the otherwise resonance-stabilized cyclic six-membered intermediate. In contrast, the fluorine atom in the axial diastereomer is gauche to both the Au(I) and the developing cationic center on C5. Additionally, this geometry aligns the σ(C4−H) and σ(C2−H) donors with the σ^*(C3−F) acceptor. The combined effect of hyperconjugation [σ(C4−H) → σ^*(C3−F), 4.4 kcal/mol; σ(C2−H) → σ^*(C3−F), 6.4 kcal/mol] and the electrostatic F/Au and F/C5 interactions significantly stabilizes TS1 (10.1 kcal/mol). Furthermore, the axial orientation disrupts the unfavorable through-bond interaction between the C−F acceptor and the cationic center in the six-membered intermediate. The importance of the gauche effect is illustrated by the near conversion of an interrupted Cope shift into its aborted version (energies relative to the starting material: equatorial intermediate, 2.9 kcal/mol; axial intermediate, 1.0 kcal/mol).

3. Curtin–Hammett Analysis of Unsubstituted and Fluorinated Substrates. For an unsubstituted substrate, the alkene group is a better donor than the allene (NBO energies: −0.4096 vs −0.4181 au) and it forms a 2 kcal/mol more stable Au(I) complex. However, comparison of the lowest-energy chair pathways for the two coordination sites (Figure 13, left) shows that the preferred product originates from the higher energy Au(I)−allene complex. The rearrangement via the more stable Au(I)−alkene complex proceeds through a higher-energy TS. The lower barrier for the Au(I)−allene pathway is explained by the higher nucleophilicity of the alkene [NBO charge at C1(TS1) = −0.40e]. In contrast, the allene moiety in the Au(I)−alkene mechanism is significantly less nucleophilic because of the hybridization differences between the targets [NBO charge at C6 (TS1) = −0.05e]. The two mechanisms are further distinguished by the nature of σ(C3−C4) fragmentation. The Au(I)−alkene mechanism has no stationary point for the cyclic six-membered intermediate and displays an inflection ("hidden TS") corresponding to the spontaneous scission of σ(C3−C4). On the other hand, the Au(I)−allene mechanism contains a well-defined cyclic intermediate that is followed by an extremely low lying TS2 (0.1 kcal/mol), indicating a nearly flat PES in this region.

With regard to the fluorinated substrate, the powerful electron-withdrawing character of fluorine significantly decreases the π basicity of the adjacent alkene by lowering the energy of the π electrons (fluorinated, −0.347 au; unsubstituted, −0.323 au). As a result, the Au(I) catalyst forms an approximately 7 kcal/mol more stable complex with the allene group (energy of π electrons = −0.328 a.u). Furthermore, hyperconjugative strengthening of the bridge C3−C4 bond interrupts the pericyclic process. The latter effect is stereoelectronic and sensitive to the alignment of C−F bonds with the vicinal donors. The pathways emanating from two modes of coordination are differentiated by the nature of the rate-limiting step. The lower-energy Au(I)−allene mechanism is characterized by the rate-limiting scission of σ(C3−C4) bridge (16.8 kcal/mol), whereas the higher-energy Au(I)−alkene mechanism is characterized by rate-determining 6-endo-trig nucleophilic attack of the allene (17.4 kcal/mol). In addition, the presence or absence of the gauche effect sets apart these two pathways by differentiating the stabilities of the six-membered intermediates: 8.3 kcal/mol for the Au(I)−alkene pathway versus 13.6 kcal/mol for the Au(I)−allene pathway (Figure 13, right).

DOI: 10.1021/jacs.5b12920
J. Am. Chem. Soc. 2016, 138, 2769−2779

SUMMARY

Coordination with cationic gold species reshapes the potential energy landscape of the allenyl Cope rearrangements. This coordination not only lowers the activation barrier but also helps to "uncouple" bond formation and bond scission, allowing the "interrupted" and "hidden-TS" mechanisms to compete with the classic concerted pericyclic pathway. For a concerted uncatalyzed allenyl Cope rearrangement, breaking of the central σ bond is a process that develops continuously along the reaction coordinate until the transition state is reached. In contrast, even the most concerted of the several available paths in the Au(I)-catalyzed version of this rearrangement involves either an inflection along the PES [in the chair Au(I)−alkene pathway] or an extremely low lying TS2 along the PES [in the chair Au(I)−allene pathway]. The inflection results from the stabilization of the geometry that would correspond to the putative second transition state. Similar dynamic features were also observed for the low-lying TS2 in the Au(I)−allene mechanism, where the rearrangement almost gives up the concertedness. Although the lowest-energy pathway involves the chair conformation and proceeds via a quasi-concerted path, alternative geometries may potentially be accessible with the proper substrate and catalyst design. Conformational effects have a large impact on the synchronicity of the rearrangement (or lack thereof). Most interestingly, a change from a chair geometry to a boat geometry can assist in preventing scission of the central σ(C3−C4) bond, potentially enabling trapping of the elusive cyclic intermediate. In these alternative pathways, the σ-bridge integrity is preserved as a result of the poor orbital overlap between the breaking bond and the nucleophilic π bond. Furthermore, an additional stabilization provided by the involvement of the terminal allenic carbon leads to the formation of a highly stable nonclassical carbocation. Potentially, the easy conversion (via a barrier of ∼0.9 kcal/mol) of the classical carbocation into the nonclassical carbocation during a Au(I)-catalyzed rearrangement can provide facile access to bridged hydrocarbons.

The incorporation of fluorine at C3 further modifies the nature of the PES. The analysis of the two lowest-energy chair pathways showed that the conformation with the axial F is preferred over the equatorial-F conformation because of σ(C−H) → σ^*(C3−F) hyperconjugation and the remote gauche effect. The introduction of the additional stereoelectronic effects due to fluorine strengthens the σ(C3−C4) bond and delays the central bond scission. As a result, the presence of fluorine at C3 interrupts the sigmatropic shift and makes the scission of the central C3−C4 bond in the cyclic intermediate the rate-limiting step in this cascade. The combination of the Au(I) catalyst and fluorine-gated stereoelectronic assistance helps to interrupt the Cope rearrangement and opens new routes for the synthesis of cyclic and polycyclic bridged hydrocarbons.

ASSOCIATED CONTENT

Supporting Information

The Supporting Information is available free of charge on the ACS Publications website at DOI: 10.1021/jacs.5b12920.

Geometries and energies of all reactants, products, and transition states and frequencies of all transition states (PDF)

AUTHOR INFORMATION

Corresponding Author

*alabugin@chem.fsu.edu

Notes

The authors declare no competing financial interest.

†Professor Marie E. Krafft, a coauthor of this article, has passed away.

ACKNOWLEDGMENTS

We are grateful to the National Science Foundation (CHE-1465142) for support of this research and to the Research Computing Center of Florida State University for the allocation of computational resources. We are grateful to Sudha Vidhani for useful discussions.

REFERENCES

(1) (a) Gilmore, K.; Manoharan, M.; Wu, J.; Schleyer, P. v. R; Alabugin, I. V. *J. Am. Chem. Soc.* **2012**, *134*, 10584. (b) Kraka, E.; Cremer, D. *Acc. Chem. Res.* **2010**, *43*, 591.

(2) (a) Roth, W. R.; Hunold, F. *Liebigs Ann. Chem.* **1996**, *1996*, 1917.

(3) (a) Jiao, H.; Nagelkerke, R.; Kurtz, H. A.; Williams, R. V.; Borden, W. T.; Schleyer, P. v. R. *J. Am. Chem. Soc.* **1997**, *119*, 5921. (b) Roth, W. R.; Gleiter, R.; Paschmann, V.; Hackler, U. E.; Fritzsche, G.; Lange, H. *Eur. J. Org. Chem.* **1998**, *1998*, 961.

(4) (a) Doering, W. v. E.; Wang, Y. *J. Am. Chem. Soc.* **1999**, *121*, 10112. (b) Doering, W. v. E.; Wang, Y. *J. Am. Chem. Soc.* **1999**, *121*, 10967. (c) Doering, W. v. E.; Birladeanu, L.; Sarma, K.; Blaschke, G.; Scheidemantel, U.; Boese, R.; Benet-Bucholz, J.; Klärner, F.-G.; Gehrke, J.-S.; Zimny, B. U.; Sustmann, R.; Korth, H.-G. *J. Am. Chem. Soc.* **2000**, *122*, 193. Also see: (d) Gentric, L.; Hanna, I.; Huboux, A.; Zaghdoudi, R. *Org. Lett.* **2003**, *5*, 3631. (e) Staroverov, V. N.; Davidson, E. R. *J. Am. Chem. Soc.* **2000**, *122*, 186. (f) Hrovat, D. A.; Beno, B. R.; Lange, H.; Yoo, H. − Y.; Houk, K. N.; Borden, W. T. *J. Am. Chem. Soc.* **1999**, *121*, 10529. (g) Hrovat, D. A.; Chen, J.; Houk, K. N.; Borden, W. T. *J. Am. Chem. Soc.* **2000**, *122*, 7456.

(5) This concept was extended to other pericyclic reactions where dynamics in the caldera region plays an important role in the observed selectivity. See: (a) Baldwin, J. E.; Keliher, E. J. *J. Am. Chem. Soc.* **2002**, *124*, 380. (b) Doubleday, C., Jr.; Suhrada, C. P.; Houk, K. N. *J. Am. Chem. Soc.* **2006**, *128*, 90.

(6) Electronic perturbations can also shift the Cope rearrangement into the dissociative regime. See: (a) Roth, W. R.; Lennartz, H.-W.; Doering, W. v. E.; Birladeanu, L.; Guyton, C. A.; Kitagawa, T. *J. Am. Chem. Soc.* **1990**, *112*, 1722. (b) Black, K. A.; Wilsey, S.; Houk, K. N. *J. Am. Chem. Soc.* **1998**, *120*, 5622. (c) Yoo, H. Y.; Houk, K. N.; Lee, J. K.; Scialdone, M. A.; Meyers, A. I. *J. Am. Chem. Soc.* **1998**, *120*, 205. (d) Black, K. A.; Wilsey, S.; Houk, K. N. *J. Am. Chem. Soc.* **2003**, *125*, 6715. (e) Carpenter, B. K. *Tetrahedron* **1978**, *34*, 1877. (f) Pal, R.; Clark, R. J.; Manoharan, M.; Alabugin, I. V. *J. Org. Chem.* **2010**, *75*, 8689.

(7) (a) Navarro-Vazquez, A.; Prall, M.; Schreiner, P. R. *Org. Lett.* **2004**, *6*, 2981. For a review, see: (b) Graulich, N.; Hopf, H.; Schreiner, P. R. *Chem. Soc. Rev.* **2010**, *39*, 1503. (c) Graulich, N. *WIREs Comput. Mol. Sci.* **2011**, *1*, 172.

(8) (a) Vidhani, D. V.; Cran, J. W.; Krafft, M. E.; Alabugin, I. V. *Org. Biomol. Chem.* **2013**, *11*, 1624. (b) Vidhani, D. V.; Cran, J. W.; Krafft, M. E.; Manoharan, M.; Alabugin, I. V. *J. Org. Chem.* **2013**, *78*, 2059. (c) Vidhani, D. V.; Krafft, M. E.; Alabugin, I. V. *Org. Lett.* **2013**, *15*, 4462. (d) Vidhani, D. V.; Krafft, M. E.; Alabugin, I. V. *J. Org. Chem.* **2014**, *79*, 352.

(9) Armstrong, A.; Boto, R. A.; Dingwall, P.; Contreras-García, J.; Harvey, M. J.; Mason, N. J.; Rzepa, H. S. *Chem. Sci.* **2014**, *5*, 2057. Roca-López, D.; Polo, V.; Tejero, T.; Merino, P. *J. Org. Chem.* **2015**, *80*, 4076. Cremer, D.; Wu, A.; Kraka, E. *Phys. Chem. Chem. Phys.* **2001**, *3*, 674. Joo, H.; Kraka, E.; Quapp, W.; Cremer, D. *Mol. Phys.* **2007**, *105*, 2697.

DOI: 10.1021/jacs.5b12920
J. Am. Chem. Soc. 2016, 138, 2769−2779

(10) Gilmore, K.; Manoharan, M.; Wu, J.; Schleyer, P. v. R.; Alabugin, I. V. *J. Am. Chem. Soc.* **2012**, *134*, 10584.
(11) Jones, R. R.; Bergman, R. G. *J. Am. Chem. Soc.* **1972**, *94*, 660.
(12) (a) Perrin, C. L.; Rodgers, B. L.; O'Connor, J. M. *J. Am. Chem. Soc.* **2007**, *129*, 4795. (b) Perrin, C. L.; Zhao, C. *Org. Biomol. Chem.* **2008**, *6*, 3349. (c) Perrin, C. L.; Reyes-Rodríguez, G. J. *J. Am. Chem. Soc.* **2014**, *136*, 15263. For a review, see: (e) Peterson, P. W.; Mohamed, R. K.; Alabugin, I. V. *Eur. J. Org. Chem.* **2013**, *2013*, 2505.
(13) For selected examples, see: Drug design: (a) Nicolaou, K. C.; Smith, A. L.; Yue, E. W. *Proc. Natl. Acad. Sci. U. S. A.* **1993**, *90*, 5881. (b) Rawat, D. S.; Zaleski, J. M. *Synlett* **2004**, *3*, 393. (c) Breiner, B.; Kaya, K.; Roy, S.; Yang, W.-Y.; Alabugin, I. V. *Org. Biomol. Chem.* **2012**, *10*, 3974. Biochemistry: (d) Galm, U.; Hager, M. H.; Van Lanen, S. G.; Ju, J.; Thorson, J. S.; Shen, B. *Chem. Rev.* **2005**, *105*, 739. Synthesis: (e) Grissom, J. W.; Gunawardena, G. U.; Klingberg, D.; Huang, D. *Tetrahedron* **1996**, *52*, 6453. Materials: (f) Chen, X.; Tolbert, L. M.; Hess, D. W.; Henderson, C. *Macromolecules* **2001**, *34*, 4104. (g) Johnson, J. P.; Bringley, D. A.; Wilson, E. E.; Lewis, K. D.; Beck, L. W.; Matzger, A. J. *J. Am. Chem. Soc.* **2003**, *125*, 14708. (h) Smith, D. W., Jr.; Shah, H. V.; Perera, K. P. U.; Perpall, M. W.; Babb, D. A.; Martin, S. J. *Adv. Funct. Mater.* **2007**, *17*, 1237. For reviews, see: (i) Kar, M.; Basak, A. *Chem. Rev.* **2007**, *107*, 2861. (j) Mohamed, R. K.; Peterson, P. W.; Alabugin, I. V. *Chem. Rev.* **2013**, *113*, 7089.
(14) "Electron-catalyzed Cope cyclizations" of substituted 1,5-hexadiene radical anions can also be considered as aborted pericyclic shifts. See: (a) Hammad, L. A.; Wenthold, P. G. *J. Am. Chem. Soc.* **2003**, *125*, 10796. (b) Chacko, S. A.; Wenthold, P. G. *J. Org. Chem.* **2007**, *72*, 494. The same is true for radical anionic Bergman cyclization. See: (c) Alabugin, I. V.; Manoharan, M. *J. Am. Chem. Soc.* **2003**, *125*, 4495.
(15) (a) Roth, W. R.; Wollweber, D.; Offerhaus, R.; Rekowski, V.; Lennartz, H.-W.; Sustmann, R.; Müller, W. *Chem. Ber.* **1993**, *126*, 2701.
(16) (a) Hrovat, D. A.; Duncan, J. A.; Borden, W. T. *J. Am. Chem. Soc.* **1999**, *121*, 169. (b) Babinski, D. J.; Bao, X.; El Arba, M.; Chen, B.; Hrovat, D. A.; Borden, W. T.; Frantz, D. E. *J. Am. Chem. Soc.* **2012**, *134*, 16139. (c) Bethke, S.; Hrovat, D. A.; Borden, W. T.; Gleiter, R. *J. Org. Chem.* **2004**, *69*, 3294. (d) Debbert, S. L.; Carpenter, B. K.; Hrovat, D. A.; Borden, W. T. *J. Am. Chem. Soc.* **2002**, *124*, 7896. (e) Duncan, J. A.; Azar, J. K.; Beathe, J. C.; Kennedy, S. R.; Wulf, C. M. *J. Am. Chem. Soc.* **1999**, *121*, 12029.
(17) (a) Barluenga, J.; Gonzalez, J. M.; Campos, P. J.; Asensio, G. *Angew. Chem., Int. Ed. Engl.* **1988**, *27*, 1546. (b) Ito, Y.; Nakatsuka, M.; Saegusa, T. *J. Org. Chem.* **1980**, *45*, 2022. (c) Curran, D. P.; Chang, C.-T. *J. Org. Chem.* **1989**, *54*, 3140. (d) Barrero, A. F.; Oltra, J. E.; Álvarez, M.; Rosales, A. *J. Org. Chem.* **2002**, *67*, 5461. (e) Stevens, R. V.; Albizati, K. F. *J. Org. Chem.* **1985**, *50*, 632. (f) Julia, M.; Colomer, E.; Julia, S. *Bull. Soc. Chim. Fr.* **1966**, 2397. (g) Julia, M.; Colomer, E. *Bull. Soc. Chim. Fr.* **1973**, 1796. (h) Siebert, M. R.; Tantillo, D. J. *J. Am. Chem. Soc.* **2007**, *129*, 8686.
(18) (a) Mauleon, P.; Krinsky, J. L.; Toste, F. D. *J. Am. Chem. Soc.* **2009**, *131*, 4513. (b) Sherry, B. D.; Toste, F. D. *J. Am. Chem. Soc.* **2004**, *126*, 15978. (c) Sherry, B. D.; Maus, L.; Laforteza, B. N.; Toste, D. *J. Am. Chem. Soc.* **2006**, *128*, 8132.
(19) Felix, R. J.; Weber, D.; Gutierrez, O.; Tantillo, D. J.; Gagné, M. R. *Nat. Chem.* **2012**, *4*, 405.
(20) (a) Henry, P. M. *Acc. Chem. Res.* **1973**, *6*, 16. (b) Henry, P. M. *Adv. Organomet. Chem.* **1975**, *13*, 363. (c) Overman, L. E. *Angew. Chem., Int. Ed. Engl.* **1984**, *23*, 579.
(21) For selected reviews of gold catalysis, see: (a) Hashmi, A. S. K. *Chem. Rev.* **2007**, *107*, 3180. (b) Nolan, S. P. *Acc. Chem. Res.* **2011**, *44*, 91. (c) Krause, N.; Winter, C. *Chem. Rev.* **2011**, *111*, 1994. (d) Li, Z.; Brouwer, C.; He, C. *Chem. Rev.* **2008**, *108*, 3239. (e) Jiménez-Núñez, E.; Echavarren, A. M. *Chem. Rev.* **2008**, *108*, 3326.
(22) Zhao, Y.; González-García, N.; Truhlar, D. G. *J. Phys. Chem. A* **2005**, *109*, 2012.
(23) (a) Tsipis, A. C.; Orpen, A. G.; Harvey, J. N. *Dalton Trans.* **2005**, 2849. (b) Zhao, Y.; Truhlar, D. G. *Org. Lett.* **2007**, *9*, 1967. (c) Reiher, M.; Salomon, O.; Hess, B. A. *Theor. Chem. Acc.* **2001**, *107*, 48. (d) Schultz, N.; Zhao, Y.; Truhlar, D. G. *J. Phys. Chem. A* **2005**, *109*, 4388. (e) Schultz, N.; Zhao, Y.; Truhlar, D. G. *J. Phys. Chem. A* **2005**, *109*, 11127. (f) Harvey, J. N. *Annu. Rep. Prog. Chem., Sect. C: Phys. Chem.* **2006**, *102*, 203.
(24) See Table 1 in the Supporting Information for the values.
(25) (a) Peng, C.; Schlegel, H. B. *Isr. J. Chem.* **1993**, *33*, 449. (b) Peng, C.; Ayala, P. Y.; Schlegel, H. B.; Frisch, M. J. *J. Comput. Chem.* **1996**, *17*, 49.
(26) (a) Reed, A. E.; Curtiss, L. A.; Weinhold, F. *Chem. Rev.* **1988**, *88*, 899. (b) Weinhold, F. In *Encyclopedia of Computational Chemistry*; Schleyer, P. v. R., Ed.; Wiley: New-York, 1998; Vol. 3, p 1792. For applications of NBO, see: (c) Glendening, E. D.; Landis, C. R.; Weinhold, F. *WIREs Comput. Mol. Sci.* **2012**, *2*, 1. (d) Weinhold, F.; Landis, C. R. *Valency and Bonding: A Natural Bond Orbital Donor–Acceptor Perspective*; Cambridge University Press: Cambridge, U.K., 2005. (e) Weinhold, F.; Landis, C. R. *Discovering Chemistry with Natural Bond Orbitals*; Wiley: Hoboken, NJ, 2012. For a representative example of the use of NBO for delocalization in transition states, see: (f) Mohamed, R.; Mondal, S.; Gold, B.; Evoniuk, C. J.; Banerjee, T.; Hanson, K.; Alabugin, I. V. *J. Am. Chem. Soc.* **2015**, *137*, 6335. (g) Mondal, S.; Gold, B.; Mohamed, R. K.; Alabugin, I. V. *Chem. - Eur. J.* **2014**, *20*, 8664.
(27) See the Supporting Information for the activation parameters corresponding to the different levels and basis sets.
(28) Frey, H. M.; Lister, D. H. *J. Chem. Soc. A* **1967**, 26.
(29) (a) Dewar, M. J. S.; Jie, C. *J. Am. Chem. Soc.* **1987**, *109*, 5893. (b) Staroverov, V. N.; Davidson, E. R. *J. Am. Chem. Soc.* **2000**, *122*, 186. (c) Doering, W. v. E; Toscano, V. G.; Beasley, G. H. *Tetrahedron* **1971**, *27*, 5299. (d) Doering, W. v. E; Troise, C. A. *J. Am. Chem. Soc.* **1985**, *107*, 5739. (e) Doering, W. v. E.; Roth, W. R. *Tetrahedron* **1962**, *18*, 67. (f) Shea, K. J.; Stoddard, G. J.; England, W. P.; Haffner, C. D. *J. Am. Chem. Soc.* **1992**, *114*, 2635.
(30) (a) Wharton, P. S.; Kretchmer, R. A. *J. Org. Chem.* **1968**, *33*, 4258. (b) Wharton, P. S.; Johnson, D. W. *J. Org. Chem.* **1973**, *38*, 4117.
(31) NBO analysis and energies of the π bonds showed that the electrons in alkene π bonds have higher energies than those in allenic π bonds.
(32) Reactant, 1.5453 Å → chair TS, 1.5929 Å; reactant, 1.5453 Å → boat TS, 1.5650 Å.
(33) (a) Castaño, O.; Palmeiro, R.; Frutos, L. M.; Luisandrés, J. *J. Comput. Chem.* **2002**, *23*, 732. (b) Metiu, H.; Ross, J.; Silbey, R.; George, T. F. *J. Chem. Phys.* **1974**, *61*, 3200. (c) Xantheas, S.; Valtazanos, P.; Ruedenberg, K. *Theor. Chim. Acta* **1991**, *78*, 327. (d) Valtazanos, P.; Elbert, S. F.; Ruedenberg, K. *J. Am. Chem. Soc.* **1986**, *108*, 3147. (e) Kumeda, Y.; Taketsugu, T. *J. Chem. Phys.* **2000**, *113*, 477. (f) Hirsch, M.; Quapp, W.; Heidrich, D. *Phys. Chem. Chem. Phys.* **1999**, *1*, 5291.
(34) (a) Wolfe, S. *Acc. Chem. Res.* **1972**, *5*, 102. (b) O'Hagan, D. *Chem. Soc. Rev.* **2008**, *37*, 308. (c) Hunter, L. *Beilstein J. Org. Chem.* **2010**, *6*, 38. (d) Zimmer, L. E.; Sparr, C.; Gilmour, R. *Angew. Chem., Int. Ed.* **2011**, *50*, 11860.
(35) (a) Tredwell, M.; Luft, J. A. R.; Schuler, M.; Tenza, K.; Houk, K. N.; Gouverneur, V. *Angew. Chem., Int. Ed.* **2008**, *47*, 357. (b) Gold, B.; Dudley, G. B.; Alabugin, I. V. *J. Am. Chem. Soc.* **2013**, *135*, 1558. (c) Gold, B.; Shevchenko, N.; Bonus, N.; Dudley, G. B.; Alabugin, I. V. *J. Org. Chem.* **2012**, *77*, 75. (d) Alabugin, I. V.; Bresch, S.; Gomes, G. d. P. *J. Phys. Org. Chem.* **2015**, *28*, 147.
(36) (a) O'Hagan, D.; Rzepa, H. S. *Chem. Commun.* **1997**, 645. (b) DeRider, M. L.; Wilkens, S. J.; Waddell, M. J.; Bretscher, L. E.; Weinhold, F.; Raines, R. T.; Markley, J. L. *J. Am. Chem. Soc.* **2002**, *124*, 2497. (c) Purser, S.; Moore, P. R.; Swallow, S.; Gouverneur, V. *Chem. Soc. Rev.* **2008**, *37*, 320.
(37) (a) Sparr, C.; Schweizer, W. B.; Senn, H. M.; Gilmour, R. *Angew. Chem.* **2009**, *121*, 3111. (b) Tanzer, E.-M.; Zimmer, L. E.; Schweizer, W. B.; Gilmour, R. *Chem. - Eur. J.* **2012**, *18*, 11334. (c) Tanzer, E.-M.; Schweizer, W. B.; Ebert, M.-O.; Gilmour, R. *Chem. - Eur. J.* **2012**, *18*, 2006. (d) Rey, Y. P.; Gilmour, R. *Beilstein J. Org. Chem.* **2013**, *9*, 2812. (e) Rey, Y. P.; Zimmer, L. E.; Sparr, C.; Tanzer, E.-M.; Schweizer, W.

DOI: 10.1021/jacs.5b12920
J. Am. Chem. Soc. 2016, 138, 2769–2779

B.; Senn, H. M.; Lakhdar, S.; Gilmour, R. *Eur. J. Org. Chem.* **2014**, *2014*, 1202. (f) Molnar, I. G.; Tanzer, E.-M.; Daniliuc, C.; Gilmour, R. *Chem. - Eur. J.* **2014**, *20*, 794.
(38) (a) Hunter, L.; O'Hagan, D. *Org. Biomol. Chem.* **2008**, *6*, 2843. (b) Farran, D.; Slawin, A. M. Z.; Kirsch, P.; O'Hagan, D. *J. Org. Chem.* **2009**, *74*, 7168. (c) Hunter, L.; Kirsch, P.; Slawin, A. M. Z.; O'Hagan, D. *Angew. Chem., Int. Ed.* **2009**, *48*, 5457. (d) Kirsch, P.; Hahn, A.; Fröhlich, R.; Haufe, G. *Eur. J. Org. Chem.* **2006**, *2006*, 4819. (e) Nicoletti, M.; Bremer, M.; Kirsch, P.; O'Hagan, D. *Chem. Commun.* **2007**, 5075.
(39) Alabugin, I. V.; Manoharan, M. *J. Org. Chem.* **2004**, *69*, 9011.
(40) In the Au(I)−allene pathway, the electrophilic Au(I)−allene complex reacts with the more nucleophilic alkene (NBO energy = −0.4096 au).
(41) (a) Goodman, L.; Gu, H.; Pophristic, V. *J. Phys. Chem. A* **2005**, *109*, 1223. (b) Rablen, P. R.; Hoffmann, R. W.; Hrovat, D. A.; Borden, W. T. *J. Chem. Soc., Perkin Trans. 2* **1999**, 1719. (c) Buissonneaud, D. Y.; van Mourik, T.; O'Hagan, D. *Tetrahedron* **2010**, *66*, 2196. (d) Baranac-Stojanovíc, M. *RSC Adv.* **2014**, *4*, 43834. (e) Fox, S. J.; Gourdain, S.; Coulthurst, A.; Fox, C.; Kuprov, I.; Essex, J. W.; Skylaris, C. K.; Linclau, B. *Chem. - Eur. J.* **2015**, *21*, 1682. (f) Sun, A. M.; Lankin, D. C.; Hardcastle, K.; Snyder, J. P. *Chem. - Eur. J.* **2005**, *11*, 1579.
(42) Briggs, C. R.; Allen, M. J.; O'Hagan, D.; Tozer, D. J.; Slawin, A. M. Z.; Goeta, A. E.; Howard, J. A. K. *Org. Biomol. Chem.* **2004**, *2*, 732.
(43) Thiehoff, C.; Holland, M. C.; Daniliuc, C.; Houk, K. N.; Gilmour, R. *Chem. Sci.* **2015**, *6*, 3565. Alabugin, I. V.; Timokhin, V. I.; Abrams, J. N.; Manoharan, M.; Ghiviriga, I.; Abrams, R. *J. Am. Chem. Soc.* **2008**, *130*, 10984.

DOI: 10.1021/jacs.5b12920
J. Am. Chem. Soc. 2016, 138, 2769−2779